Fibers and Polymers 2003, Vol.4, No.3, 135-144

Permeability Measurement of a Circular Braided Preform for Resin Transfer Molding

Yun Kyoung Cho, Young Seok Song, Tae Jin Kang, Kwansoo Chung, and Jae Ryoun Youn*

School of Materials Science and Engineering, Seoul National University, Seoul 151-742, Korea
(Received July 29, 2003; Revised September 1, 2003; Accepted September 8, 2003)

Abstract: Permeability of the preform is one of key factors in design of RTM (Resin Transfer Molding) mold, determination of processing conditions, and modeling of flow in the mold. According to previous studies, permeability measured in the unsaturated fiber mats are higher than that in the saturated fiber mats by about 20 % because of the capillary pressure. In this study, permeabilities of several fiber preforms are measured for both saturated and unsaturated flows. A saturated experiment of radial flow has been adopted to measure the permeability of anisotropic fiber preforms with high fiber content, i.e., circular braided preforms. In this method, four pressure transducers are used to measure the pressure distribution. Permeabilities in different directions are determined and the experimental results show a good agreement with the theory. Since permeability is affected by the capillary effect, permeability should be measured in the unsaturated condition for the textile composites to be manufactured under lower pressure as in the Vacuum Assisted Resin Transfer Molding (VARTM).

Keywords: Permeability, Circular braided preform, Resin transfer molding, Saturated flow, Unsaturated flow

Introduction

Resin Transfer Molding (RTM) is a versatile and efficient process for producing fiber reinforced polymer composites, which have either small structures of simple shape or large structures of complex shape [1,2]. It enables us to make various parts with large volume and high performance at low cost. The RTM process can be broadly divided by following steps. The first step is to place a preform in the mold cavity. The fiber preforms are usually constructed from woven or non-woven fiber mats, which are frequently made of continuous strand fibers of glass and aramid. The fiber preform will provide the finished piece with the majority of its structural properties. Once the mold for RTM has been sealed, a polymeric resin is injected into the mold cavity, saturates the preform and expels any air present. After complete filling of the mold cavity, curing reaction is initiated and the part is solidified. The finished composite product is removed from the mold when gelation of the resin is accomplished.

In the RTM process, the capillary pressure exists only in flow-front region and it is negligible in resin-filled region [3-5]. Therefore, the permeability measurement for the RTM process should be performed under the saturated state for the effect of capillary pressure to be eliminated. In order to improve the permeability measurement for the fiber mats with high fiber contents, a measurement technique for the permeability is developed in this study. The measurement technique for planar permeability is similar to that used by Adams *et al.* [6-8]. The major differences between the two measurement methods are [9]:

(1) the measurement is carried out at steady-state with resin flow through a fully saturated fiber mat.

(2) pressures at four locations in the flow field, instead of flow front locations, are measured and used for determination of the permeabilities.

Accurate permeability data are needed for numerical simulation of resin flow in order to design the RTM mold [10-12] and predict the resin flow in the mold [13,14]. In this study, permeabilities of three different fiber mats, such as random glass mat, aramid plain woven fabric and circular braided preform, are measured for the unidirectional and radial flow. The unsaturated and saturated permeability values are obtained experimentally and the results are compared. Because the braided preform is anisotropic, the shape of flow front is elliptic. The permeability for the braided preform is obtained through the saturated and unsaturated radial flow experiments.

Theory

Unidirectional Flow

Permeability represents resistance against fluid flow through porous media and is described in terms of Darcy's law [1,2]

$$\bar{u} = -\frac{K}{\mu}\nabla P \tag{1}$$

where $\bar{u}$: Darcy's velocity vector

μ: Newtonian viscosity of the fluid

∇P : pressure gradient vector

K: permeability tensor of the porous medium

In the case of one-dimensional flow experiments, the fluid flows through the preform in one direction. After the mold cavity is completely filled with fluid, steady-state data are collected by measuring the flow rate and the pressure drop along the flow direction. After a number of data points are collected, steady-state flow rate is plotted as a function of

*Corresponding author: jaeryoun@snu.ac.kr

steady-state pressure gradient. If the Newtonian fluid is used in the experiment, a linear relationship should be obtained between the flow rate and the pressure gradient. Darcys law indicates that the slope of such a line is proportional to the ratio of permeability to the viscosity. Components of the in-plane principal permeability tensor can be obtained from the unidirectional flow experimental data if at least two experiments are conducted in the principal directions. Two pressure transducers were located in the mold to measure the pressure gradient between two points. The permeability of each fiber preform was calculated by using the following equation [15-17].

$$K = -\frac{\bar{u}\mu}{\nabla P} = -\frac{V\mu}{At\nabla P} = \frac{V\mu\delta}{At(P_1 - P_2)} \quad (2)$$

where V: volume of fluid
A: cross-sectional area of the mold
t: elapsed time
P_1, P_2: pressure at pressure transducer 1, 2
d: distance between two pressure transducers (= 0.2 m)

Radial Flow

Isotropic Preform

The radial velocity in the radial flow experiment is expressed by Darcy's law written for radial flow:

$$v_r = -\frac{K_{rr}\partial P}{\mu\ \partial r} \quad (3)$$

Equation (3) is obtained by solving the Laplace's equation in polar coordinates. By substituting the new pressure distribution into the equation (3) and integrating the equations by using the boundary conditions $\varepsilon(dr_f/dt) = v$ at the flow front and $r_f = r_0$ at $t = 0$, the permeability is obtained as follows [7].

$$K = \{r_f^2[2\ln(r_f/r_0) - 1] + r_0^2\}\frac{1}{t}\frac{\mu\varepsilon}{4\Delta P} \quad (4)$$

where ε is the porosity, μ is the dynamic viscosity of the fluid, t is the elapsed time after injection, and r_f and r_0 are the radii of the flow front and inlet. ΔP is the difference between the pressure at the flow front P_f and the inlet pressure P_0. The inlet pressure is usually measured as the pressure above the ambient pressure. Hence, ΔP is equal to the pressure applied at the inlet. The radius r is related to the x, y coordinates by $r = \sqrt{x^2 + y^2}$. Equation (4) can be used to compute the permeability from radial flow tests for isotropic materials at constant inlet pressure.

In the experiment the flow front radius r_f is measured at different time steps while the other parameters are kept constant. The term in the curly brackets in the equation (4) is plotted versus time for the different flow front steps and the gradient of the regression line is called F_{iso} [18]. Permeability is obtained by the following equation.

$$K = F_{iso}\frac{\mu\varepsilon}{4\Delta P} \quad (5)$$

Equation (5) shows that the gradient F_{iso} is constant for every flow front position because μ, ε and ΔP as well as K are constant throughout the experiment. In other words, the regression line fitted to the experimental data should go through the origin.

Anisotropic Preform

For fabrics commonly used in RTM, elliptical flow fronts are observed because the second order partial differential equation of the pressure distribution is no longer Laplace's equation

$$K_1\frac{\partial^2 P}{\partial x^2} + K_2\frac{\partial^2 P}{\partial y_2} = 0 \quad (6)$$

where K_1 and K_2 are the two principal permeabilities. It is possible to obtain an analytical solution for the equation (6). It can be achieved by transforming the physical domain into a quasi-isotropic system by applying the following transformation.

$$x' = x\alpha^{1/4} \quad y' = y\alpha^{-1/4} \quad \text{with} \quad \alpha = \frac{K_2}{K_1} \quad (7)$$

where α is also called the degree of anisotropy. The quasi-isotropic permeability is defined as

$$K' = \sqrt{K_1 K_2} \quad (8)$$

while the radius in the quasi-isotropic system is $\bar{r} = \sqrt{x'^2 + y'^2}$.

The quasi-isotropic radii of the flow front measured in the direction of the two principal axes, $\bar{r}_{f,I}$ and $\bar{r}_{f,III}$, are

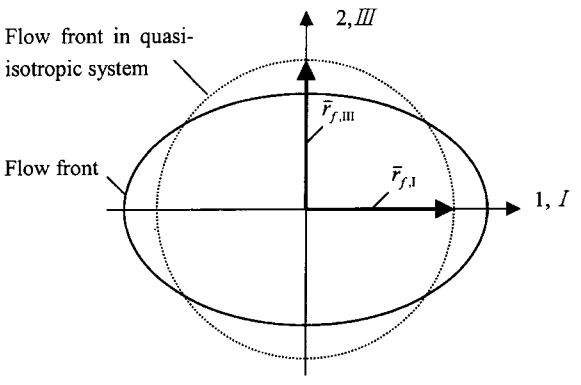

Figure 1. Transformation of the flow front to the quasi-isotropic system.

shown in Figure 1. The inlet radii are transformed by the same way. The quasi-isotropic permeability is defined as follows for anisotropic materials [18].

$$K' = \left\{\left(\left(\frac{K_2}{K_1}\right)^{1/2} x_f^2 + \left(\frac{K_1}{K_2}\right)^{1/2} y_f^2\right) \left[2\ln\left(\left(\left(\frac{K_2}{K_1}\right)^{1/2} x_f^2 + \left(\frac{K_1}{K_2}\right)^{1/2} y_f^2\right)^{1/2} \Big/ \left(\left(\frac{K_2}{K_1}\right)^{1/2} x_0^2 + \left(\frac{K_1}{K_2}\right)^{1/2} y_0^2\right)^{1/2}\right) - 1\right] + \left(\left(\frac{K_2}{K_1}\right)^{1/2} x_0^2 + \left(\frac{K_1}{K_2}\right)^{1/2} y_0^2\right)\right\} \frac{1}{t} \frac{\mu\varepsilon}{4\Delta P} \quad (9)$$

where x_f and y_f are the flow front radii and x_0 and y_0 are the inlet radii. Although the expression for K' has become quite complex, there exist two preferred orientations where the equation (9) is simplified significantly. An explicit solution for K_1 is obtained by setting y_0 and y_f in the equation (9) to be zero, substituting the equation (8) into the left hand side of the equation (9), and multiplying both sides of the equation (9) with the square root of the inverse of α.

$$K_1 = \{x_f^2[2\ln(x_f/x_0) - 1]x_0^2\} \frac{1}{t} \frac{\mu\varepsilon}{4\Delta P} \quad (10)$$

A closed form solution for K_2 is obtained in a similar manner.

$$K_2 = \{y_f^2[2\ln(y_f/y_0) - 1]y_0^2\} \frac{1}{t} \frac{\mu\varepsilon}{4\Delta P} \quad (11)$$

Again, the straight line fitted to the terms in the curly brackets of the equations (10) and (11) versus time has a constant gradient.

Planar Permeability Measurement for Anisotropic Fiber Preform

Equation (6) can be transformed to the following equation as depicted in Figure 2 by introducing $x' = x\alpha^{1/4}$, $y' = y\alpha^{-1/4}$, and $p' = (p - p_r)/(p_0 - p_r)$

$$\frac{\partial^2 p'}{\partial x'^2} + \alpha \frac{\partial^2 p'}{\partial y'^2} = 0 \quad (12)$$

where p_0 is the inlet pressure and p_r is the pressure at a reference point.

As the result of the transformation, the inlet circle becomes an ellipse. To implement the boundary conditions on the ellipse, an elliptical coordinate system is used. The relationship between the elliptical coordinates (ξ, η) and the rectangular coordinates (x', y') can be written as

$$x' = L\cosh\xi\cos\eta \quad (13\text{-a})$$

$$y' = L\sinh\xi\sin\eta \quad (13\text{-b})$$

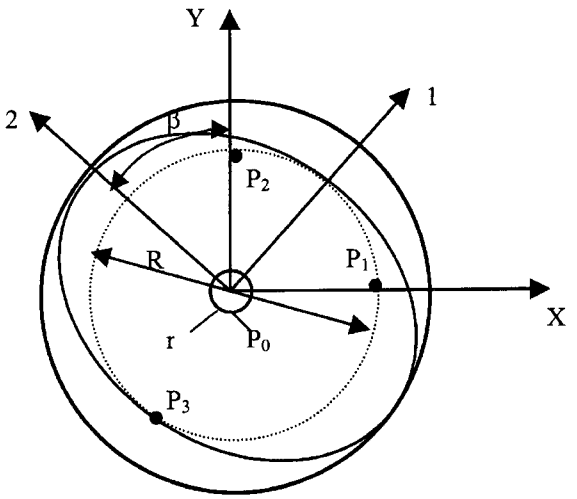

Figure 2. Location of four pressure transducers.

where $L = r_0(\alpha^{-1/2} - \alpha^{1/2})^{1/2}$ is one half of the focal length of the inlet ellipse.

By knowing the flow rate and the pressures at four locations, p_0, p_1, p_2, and p_3, as shown in Figure 2, one can determine the permeabilities in the two principal directions, K_1, K_2, and the angle, β, between the principal direction of the fiber preform and the global coordinate.

Locations of the pressure transducers in the elliptical coordinates are [9]

$$\xi_0 = \ln\left[\frac{1 + \alpha^{1/2}}{(1 - \alpha)^{1/2}}\right] \quad (14\text{-a})$$

$$\xi_1 = \ln\left[\sqrt{\left(\frac{x_1}{x_0} \cdot \frac{1}{\sqrt{1 - \alpha}}\right)^2 - 1} + \frac{x_1}{x_0} \cdot \frac{1}{\sqrt{1 - \alpha}}\right] \quad (14\text{-b})$$

$$\xi_2 = \ln\left[\sqrt{\left(\frac{y_2}{y_0} \cdot \frac{\sqrt{\alpha}}{\sqrt{1 - \alpha}}\right)^2 + 1} + \frac{y_2}{y_0} \cdot \frac{\sqrt{\alpha}}{\sqrt{1 - \alpha}}\right] \quad (14\text{-c})$$

The dimensionless flow rate, q_d, can be obtained by using Darcy's law [19]:

$$q_d = \frac{q\mu}{K'h(p_0 - p_r)} = \int_0^{2\pi} \frac{dp'}{d\xi}\Big|\xi = \xi_r d\eta \quad (15)$$

where q is the injected flow rate (m^3/s), μ is the liquid viscosity (Pa·s), and h is the preform thickness (m). It is assumed that pressure is a function of ξ in the elliptical coordinate system as shown below.

$$p' \approx \frac{\xi_r - \xi}{\xi_r - \xi_0} \quad (16)$$

Integration of the equation (15) yields the following equation.

$$(\xi_r - \xi_0) - \frac{2\pi h(p_0 - p_r)}{q\mu} K' = 0 \qquad (17)$$

Substituting the equation (14) into equation (17) results in two nonlinear equations.

$$\ln\left[\sqrt{\left(\frac{x_1}{x_0}\frac{1}{\sqrt{1-\alpha}}\right)^2} - 1 + \frac{x_1}{x_0}\frac{1}{\sqrt{1-\alpha}}\right] - \ln\left[\frac{1+\alpha^{1/2}}{(1-\alpha)^{1/2}}\right] - \frac{2\pi h(p_0-p_1)}{q\mu}K' = 0 \qquad (18\text{-a})$$

$$\ln\left[\sqrt{\left(\frac{y_1}{y_0}\frac{\sqrt{\alpha}}{\sqrt{1-\alpha}}\right)^2} + 1 + \frac{y_1}{y_0}\frac{\sqrt{\alpha}}{\sqrt{1-\alpha}}\right] - \ln\left[\frac{1+\alpha^{1/2}}{(1-\alpha)^{1/2}}\right] - \frac{2\pi h(p_0-p_2)}{q\mu}K' = 0 \qquad (18\text{-b})$$

where $\alpha = K_2/K_1$ and $K' = \sqrt{K_1 K_2}$. Solving the two nonlinear equations for α and K' yields the in-plane permeabilities K_1 and K_2. By using equation (17), ξ_3 can be obtained. With ξ_3 and equation (18-a) or (18-b), the angle β can then be obtained [9].

Experiments

Materials

Fiber Preform

Three different fiber preforms were used in this study, which were glass fiber random mats, aramid fiber woven fabrics and glass fiber braided preform. Particularly, the braided preform was prepared by using a 3-D braiding machine. In the 4-step braiding process, the braider yarns are intertwound through their relative displacements. The braiding machine has 1 × 1 braiding pattern because of the identical travel distance in the direction of rows or columns per each step. The basic carrier motion of the process is illustrated in Figure 3. The basic machine bed consists of 4 × 6 carriers. The fiber tows are arranged in rows and columns to form the required shape and then additional tows are added to the outside of the array at alternating locations. Four motion steps of the carriers constitute one machine cycle. In step 1, the rows of the basic machine bed move alternately in a horizontal direction (first and third rows move to the left and second and fourth rows move to the right). In step 2, the columns of the basic machine bed move alternately in the vertical direction (first, third, and fifth columns move down and second, fourth, and sixth columns move up). In step 3, the movements of the rows are similar to those in step 1, but the directions are opposite. In step 4, the movements of the columns are similar to those in step 2, but the directions are again opposite. At the end of the four steps (i.e., one machine cycle), the yarn carrier arrangement is the same as the initial configuration, although individual carriers have changed their positions. As the four steps are repeated the tows move throughout the cross-section and are interlaced to form the braided structure [19,20].

In this study, multi-axial braided preforms were produced by using the circular braiding machine with 48 carriers and with provision for 12 axial tows. Carriers of the braiding machine were moved by pneumatic cylinders using compressed

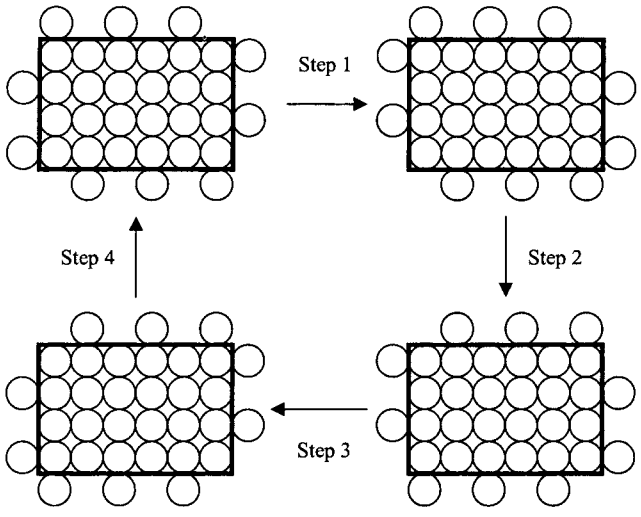

Figure 3. The four step 1 × 1 braiding pattern (Basic machine bed: $m \times n = 6 \times 4$).

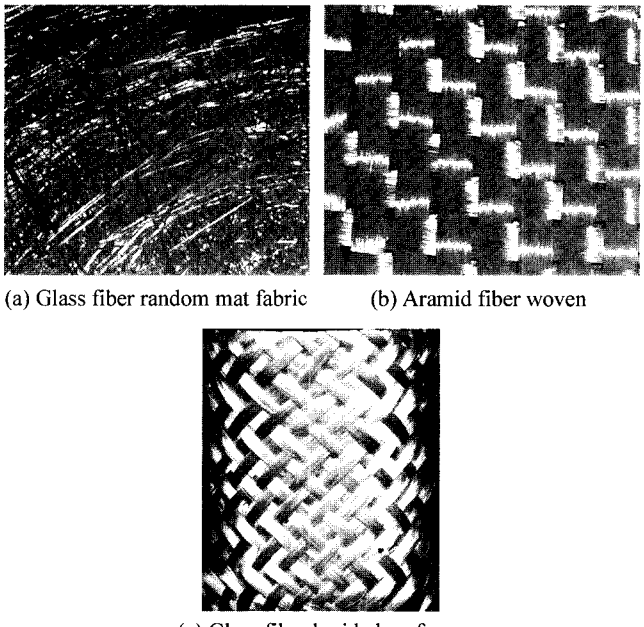

(a) Glass fiber random mat fabric (b) Aramid fiber woven

(c) Glass fiber braided preform

Figure 4. Fiber preforms used in the experiment.

Table 1. Density and volume fraction of different performs used for experiments

Properties / Fibeer preform	ρ_f (g/cm^3)	ρ_m (g/cm^3)	V_f^*
Glass random mat	2.5	0.495	0.198
Aramid fabric	1.4	0.420	0.3
Braided preform	2.5	1.45	0.58
		1.65	0.66
		1.875	0.75

air. E-glass roving yarns were used for braiding and braided preforms are shown in Figure 4.

Permeability is a strong function of porosity. In order to specify the porosity, the volume fraction of fiber preform should be determined. Volume fraction of fiber preform was calculated by using the following equation.

$$V_f^* = \frac{\rho_m}{\rho_f} \tag{19}$$

where V_f^*: volume fraction of fiber preform
ρ_f: density of fiber
ρ_m: density of mat

Densities and volume fractions of the fiber preforms are listed in Table 1.

Resin

Silicone oil (dimethyl siloxane polymer, DC 200F/100CS) supplied from Dow Corning was used as the injection fluid. It is assumed that the silicone oil shows Newtonian behavior so that the Darcy's law can be applied. Its viscosity is 9.7×10^{-2} Pa·s.

Experimental Apparatus

Mold Design

(1) Unidirectional flow experiment

Experimental apparatus was designed and constructed for measuring permeability and observing mold filling behavior. A transparent mold was constructed by using a acrylic (PMMA) plate to observe mold filling pattern visually. A digital camcorder was used in order to visualize flow advancement. Two pressure transducers were located in the mold to measure the pressure difference. To prevent the leakage of resin from the mold, O-rings were installed between the top and bottom plates of the mold. Bolts, nuts and C-clamps were used to minimize the gap between the top and bottom parts of the mold by applying pressure. The schematic diagram of the mold [21,22] is presented in Figure 5.

(2) Radial flow experiment

Architecture of the mold used to obtain two-dimensional flow data is illustrated in a simplified schematic diagram in Figure 6. A radial in-plane flow was generated by injecting the fluid through a central gate into the preform which is placed in a space between two parallel plates. Top and bottom plates were made of steel and the transparent plate was made of PMMA which is transparent for observation of the flow. A digital camcorder was also used in order to visualize flow pattern. Four pressure transducers were located in the mold to measure pressure drop at each position.

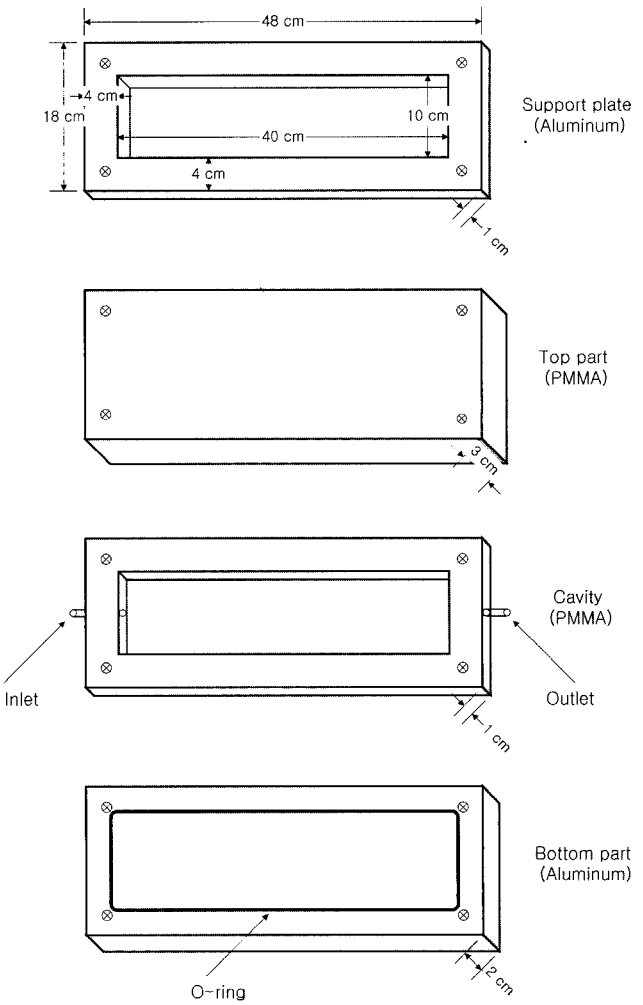

Figure 5. Schematic diagram of the mold used in the unidirectional flow experiment.

Experimental Set-up

The experimental set-up is shown schematically in Figure 7. The experimental set-up enabled us to measure permeability in the two cases, unidirectional and radial flow experiments. The resin was injected into the mold under constant pressure. Pressure transducers were used to measure the pressure of liquid at the inlet and other locations. A data acquisition

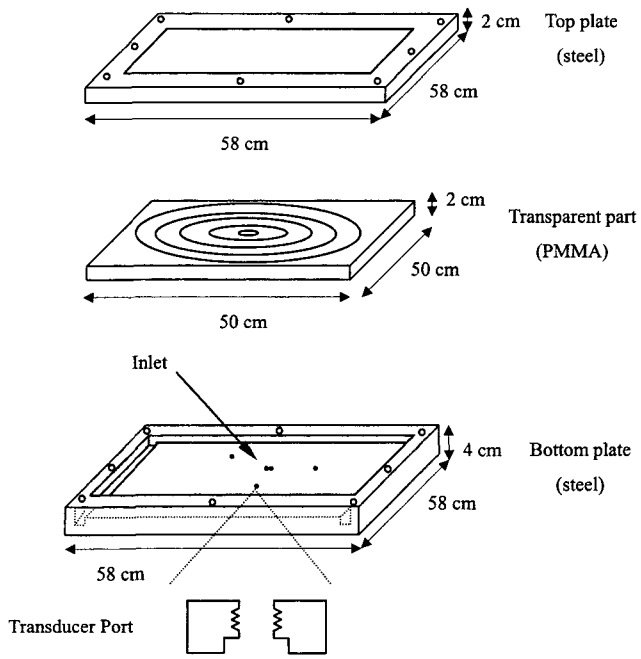

Figure 6. Schematic diagram of the mold used in the radial flow experiment.

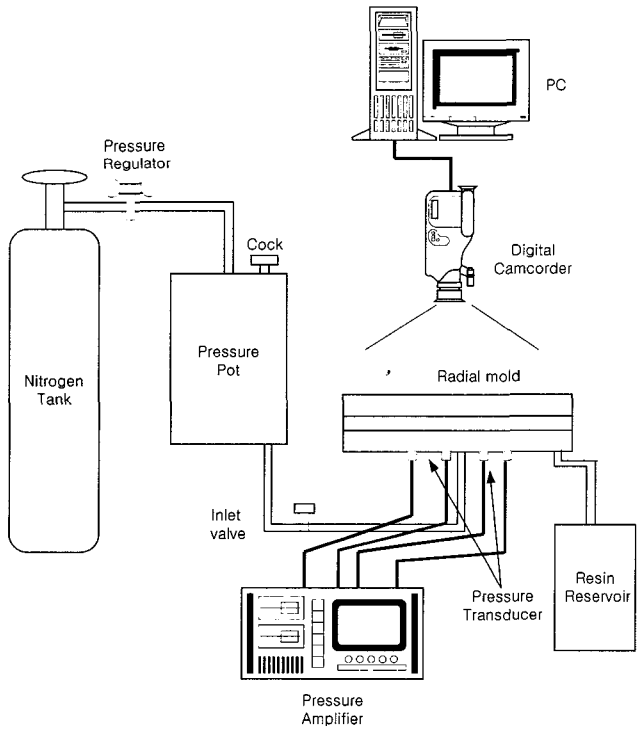

Figure 7. Schematic diagram of the experimental setup for the study of resin transfer molding.

system collected the pressure and the elapsed time. Using the two different molds, the permeability measurement was performed for the two cases. Permeability was measured at different fiber volume fractions by compressing the fiber mat to different extent. Compressed nitrogen gas was used for injection of the resin into the mold. Pressures were monitored at the four locations continuously. Pressure values were recorded after the preform had been wetted out completely and the system had reached the steady state. Then equations (6), (10), and (11) were used to calculate the permeabilities, K_1 and K_2.

Measurement of Inplane Permeability

The in-plane permeabilities of three different fiber preforms, glass fiber random mats, aramid fiber woven fabrics and glass fiber braided preforms, were measured. Volume fraction of each preform was specified experimentally. Each experiment was performed under the constant inlet pressure. Silicone oil (DC 200F) was used as an injecting fluid, whose viscosity is 9.7×10^{-2} Pa·s.

For glass fiber random mats and aramid fiber plain woven fabrics, saturated test of unidirectional flow and unsaturated test of radial flow were carried out. Pressure was applied by compressed nitrogen in the range of 0.25 to 0.26 MPa. Pressure gradient was calculated from measured values at two different pressure transducers. Volumetric flow rate was calculated by measuring volume of fluid and time. The measured average flow rate was in the range of 1.79 to 6.28 m^3/s. From these experimental data, the in-plane permeability of the single layered fiber preform was calculated through the Darcys law. Advancement of flow front was also observed by using a digital camcorder.

Permeability measurements of the braided preform were carried out by using saturated and unsaturated tests of radial flow under constant pressure. Flat braided preform acquired by unfolding a cylindrical preform of 80 mm diameter was placed in the mold cavity and compressed by the mold plates to control thickness of the cavity. Radial in-plane flow was achieved by injecting the fluid into the cavity through a central gate. A 20 mm-thick transparent plate on which concentric circles were drawn was used to record the advancement of the flow front with digital camcorder. Pressures at four locations in the cavity were measured and used for determination of the permeabilities.

Results and Discussion

Glass Fiber Random Mats and Aramid Fiber Plain Woven Fabrics

Unsaturated Permeability

The glass random mats used in the experiment have fiber density of 2.5 g/cm^3 and porosity of 0.81. The aramid fiber fabrics have fiber density of 1.4 g/cm^3 and porosity of 0.7. Unsaturated permeability was determined by the radial flow measurement under constant pressure. The inlet pressure

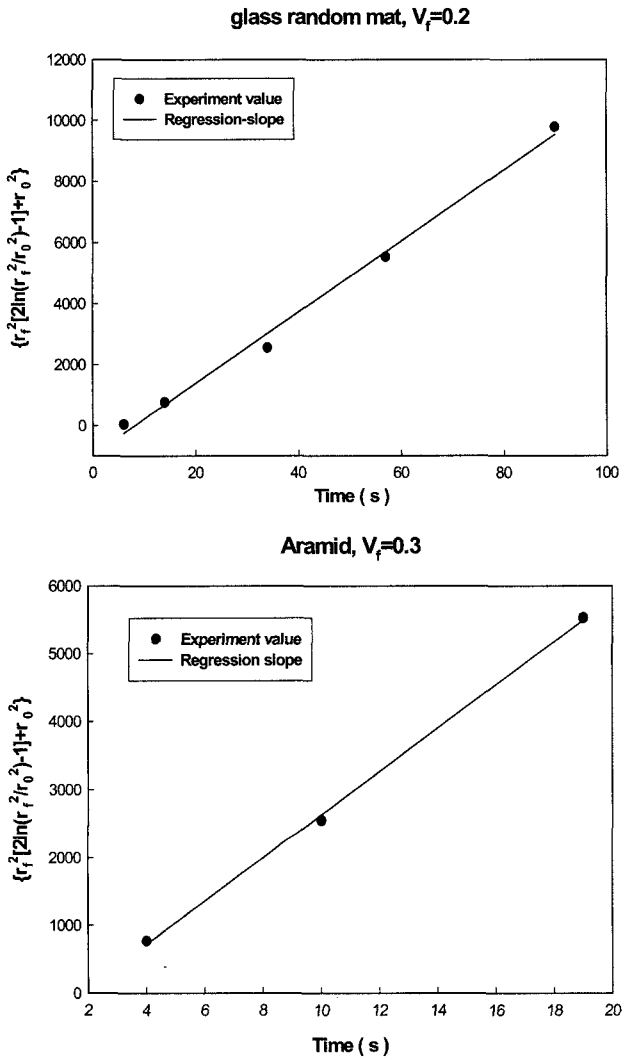

Figure 8. Curve fitting of the flow front as a function of time for glass random mats and aramid plain woven fabrics.

Table 2. Experimental results of the unsaturated permeability

	Glass random mat	Aramid fabric
Porosity	0.8	0.7
P ($\times 10^5$ Pa) (inlet pressure)	0.3	0.15
K_{rr} ($\times 10^{-9}$ m^2)	3.0	1.2

was measured by pressure transducers located in the mold. Permeability of each fiber preform was calculated by the equation (9). From the slope of the regression line in Figure 8, the unsaturated permeability is obtained as shown in Table 2 by the equations (10) and (11).

Saturated Permeability

Volume flow rate was determined by measuring the volume of injected fluid with the exact elapsed time. In order to compare the permeabilities of different preforms, porosity used in the experiment was the same. Pressures were measured at two pressure transducers located in the mold designed for the unidirectional flow test. Permeability of each fiber preform with respect to the volume fraction is listed in Table 3. Capillary effects can be examined by comparing the results of unsteady and steady permeability measurements. Despite of the edge effects which are usually met in the unidirectional flow experiment, the saturated permeability is lower than the unsaturated permeability because of the capillary effect in the unsaturated preform. In particular, the difference between the saturated and unsaturated permeabilities is larger in the case of glass random mats. Because the structure of aramid fiber plain woven fabrics is coarse, capillary effect will be lower than that of the glass fiber random mats.

Table 3. Experimental results of the saturated permeability

	Glass random mat	Aramid plain woven fabrics
ε	0.82	0.700
V (cm^3)	291	176
T (s)	65.34	140.60
P_1 ($\times 10^5$ Pa)	1.517	2.275
P_2 ($\times 10^5$ Pa)	1.034	3.585
K_{rr} ($\times 10^{-9}$ m^2)	1.7902	1.1740

Braided Preform

Unsaturated Permeability

The similar procedure was repeated to determine the unsaturated permeability for braided preform. Because the braided preform has anisotropic structure, shape of the flow front is elliptical. In the flattened preform, machine direction is referred to as x axis and circumferencial direction is identified as y axis. Mold filling pattern for the braided preform is shown Figure 9. Unsaturated permeabilities in the principal direction were obtained in Figure 10 by using the equations (10) and (11). Unsaturated permeabilities were obtained in the case of various porosity, 0.58, 0.66, and 0.75 as shown in Table 4. In order to observe the capillary effect, experiments were carried out for the same porosity. Because capillary effects can be neglected under high pressure, permeability under high pressure gradient is lower than that under low pressure gradient.

Saturated Permeability

In order to measure the permeability accurately, An experimental method for saturated radial flow was carried out for the braided preform. Instead of two point pressure measurement, pressure was measured at four locations to calculate the permeability. The two nonlinear equations

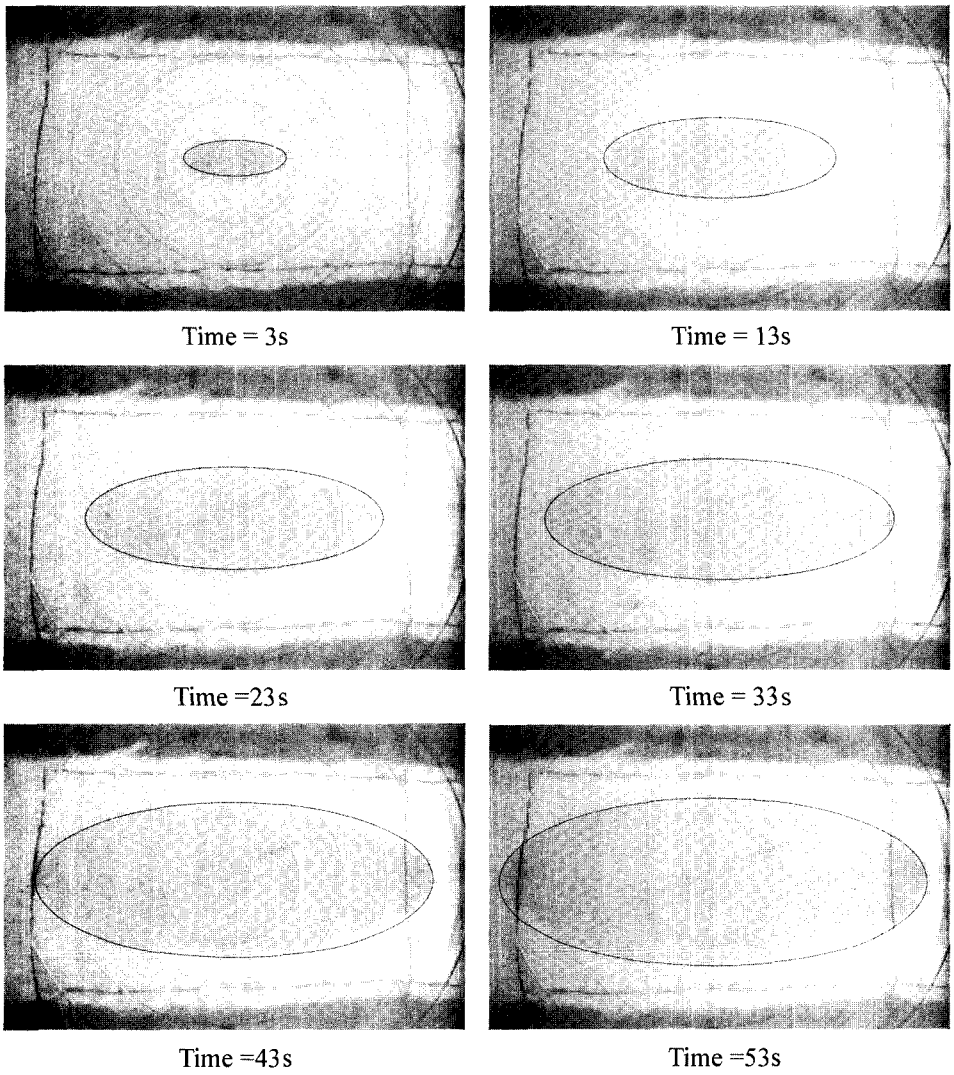

Figure 9. Advancement of the resin flow front in glass preform.

Table 4. Experimental results of the unsaturated permeability obtained for the the braided preform

Porosity	0.58	0.66	0.75	0.65
Pressure ($\times 10^5$ Pa)	0.5	0.35	0.21	0.6
Viscosity (Pa·s)		9.7×10^{-2}		
x-dir slope ($\times 10^{-3}$)	3.68169	12.129	13.328	17.706
y-dir slope ($\times 10^{-3}$)	0.60368	2.3456	2.5986	3.5018
K_{xx} ($\times 10^{-9}$ m^2)	1.036	5.547	11.54	4.652
K_{yy} ($\times 10^{-9}$ m^2)	0.1698	1.073	2.251	0.92

(equation (18)) are solved and then α and K' are obtained (Figure 11).

The experimental results are shown in Table 5. Comparison of the saturated and unsaturated permeabilities is shown in Figure 12. The unsaturated permeability also has higher values. In the case of lower porosity, the saturated permeability in the y direction is slightly higher than the unsaturated permeability. Because of the small yarn orientation angle (26°) against the mandrel axis, direction of main flow is almost perpendicular to the yarn direction of the preform and the capillary effect will play less important role in the direction of dominant flow.

Conclusions

Permeabilities of three different preforms, glass fiber random mats, aramid fiber plain woven fabrics and glass fiber braided preforms, are measured by using unidirectional and radial flow experiments. Due to the isotropic structure of glass random mats and aramid plain woven fabrics, their saturated permeabilities are measured by using the mold

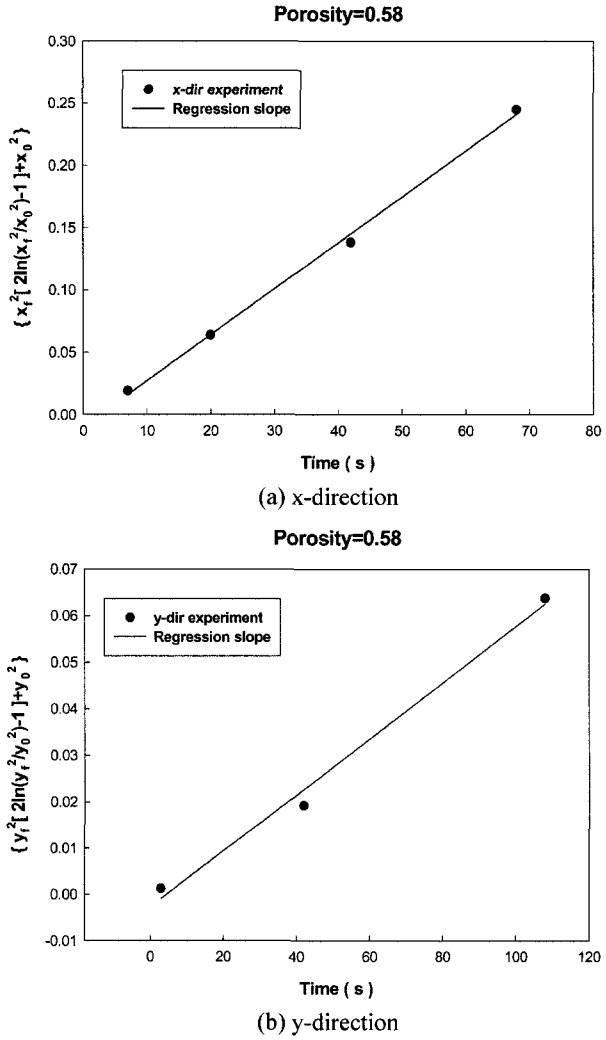

(a) x-direction

(b) y-direction

Figure 10. Curve fitting of the flow front as a function of time for Braided preform (porosity = 0.58).

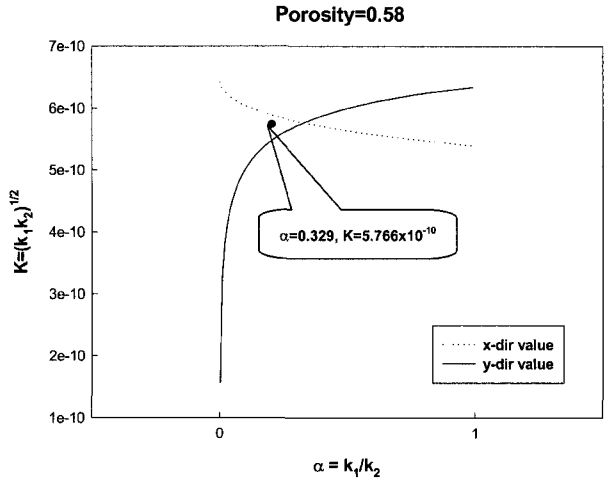

Figure 11. Solution of the two nonlinear equations when the porosity is 0.58.

Table 5. Experimental results of saturated permeability obtained for the braided preforms

Porosity	0.58	0.66	0.75
α	0.329	0.18982	0.21979
K ($\times 10^{-9}$ m^2)	0.5766	2.36	4.69
k_{xx} ($\times 10^{-9}$ m^2)	1.005	5.417	10.0
k_{yy} ($\times 10^{-9}$ m^2)	0.33	1.028	2.199

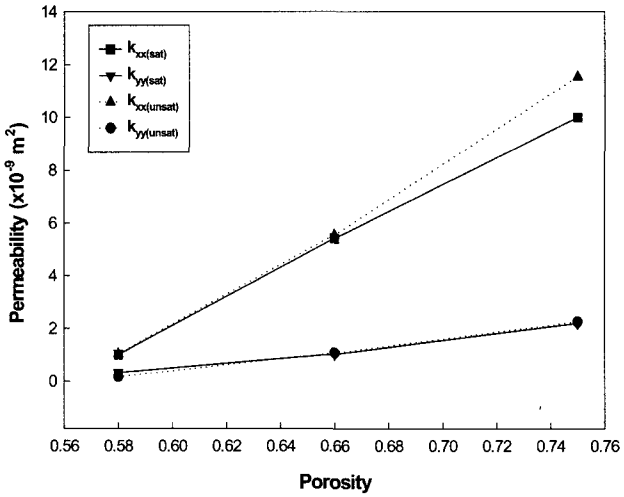

Figure 12. Comparision of the unsaturated and saturated permeability with respect to porosity.

designed for the unidirectional flow experiment. Unsaturated permeabilities are obtained by using the mold designed for the radial flow experiment. Because of the capillary pressure, the permeability measured for unsaturated fiber mats is higher than that for saturated fiber mats by 3 to 40 %. Multi-axial Braided preforms prepared by using the 3-D circular braiding machine are used to measure the saturated and unsaturated permeabilities with the mold designed for the radial flow experiment. An experimental method for measuring in-plane permeabilities of anisotropic fiber preforms has been developed. The experimental technique requires pressure measurement at the steady state of radial flow through a fully saturated fiber mat. Permeability is affected by the capillary pressure and measurement of permeability is critical when polymer composites are manufactured under lower pressure.

Acknowledgements

This study was partially supported by the Korea Science and Engineering Foundation through the Applied Rheology Center (ARC) and by the Ministry of Science and Technology through the National Research Laboratory. The authors are grateful for the support.

References

1. S. G. Advani, M. V. Bruschke, and R. S. Parnas, "Flow and Rheology in Polymer Composites Manufacturing", Elsevier, Amsterdam, 1994.
2. R. A. Greenkorn, "Flow Phenomena in Porous Media", Marcel Dekker, New York, 1983.
3. K. L. Ahn and J. C. Seferis, *Polym. Compos.*, **12**, 146 (1991).
4. W. B. Young, *J. Compos. Mater.*, **30**, 1191 (1996).
5. S. Amico and C. Lekakou, *Compos. Sci. Technol.*, **61**, 1945 (2001).
6. K. L. Adams and L. Rebenfeld, *Polym. Compos.*, **12**, 179 (1991).
7. K. L. Adams, W. B. Russel, and L. Rebenfeld, *Int. J. Multiphase Flow*, **14**, 203 (1988).
8. K. L. Adams and L. Rebenfeld, *Polym. Compos.*, **12**, 186 (1991).
9. K. K. Han, C. W. Lee, and B. P. Rice, *Compos. Sci. Technol.*, **60**, 2435 (2000).
10. R. S. Parnas, K. M. Flynn, and M. E. Dal-Favero, *Polym. Compos.*, **18**, 623 (1997).
11. Y. Luo, I. Verpoest, K. Hoes, M. Vanheule, H. Sol, and A. Cardon, *Compos. Part A- Appl. Sci.*, **32**, 1497 (2001).
12. Y. H. Lai, B. Khomami, and J. L. Kardos, *Polym. Compos.*, **18**, 368 (1997).
13. R. Gauvin, F. Trochu, Y. Lemenn, and L. Diallo, *Polym. Compos.*, **17**, 34 (1996).
14. H. Golestanian and A. S. El-Gizawy, *Polym. Compos.*, **19**, 395 (1998).
15. A. W. Chan and S. T. Hwang, *Polym. Eng. Sci.*, **31**, 1233 (1991).
16. R. S. Parnas and A. J. Salem, *Polym. Compos.*, **14**, 383 (1993).
17. T. J. Wang, C. H. Wu, and L. J. Lee, *Polym. Compos.*, **15**, 278 (1994).
18. J. R. Weitzenböck, R. A. Shenoi, and P. A. Wilson, *Compos. Part A- Appl. Sci.*, **30**, 781 (1999).
19. Z. X. Tang and R. Postle, *Compos. Struct.*, **49**, 451 (2000).
20. A. C. Long, *Compos. Part A- Appl. Sci.*, **32**, 941 (2001).
21. D. G. Seong, K. Chung, T. J. Kang, and J. R. Youn, *Polym. Polym. Compos.*, **10**, 493 (2002).
22. Y. S. Song, K. Chung, T. J. Kang, and J. R. Youn, *Polym. Polym. Compos.*, **11**, in press (2003).